N O T I C E

THIS DOCUMENT HAS BEEN REPRODUCED FROM MICROFICHE. ALTHOUGH IT IS RECOGNIZED THAT CERTAIN PORTIONS ARE ILLEGIBLE, IT IS BEING RELEASED IN THE INTEREST OF MAKING AVAILABLE AS MUCH INFORMATION AS POSSIBLE

NASA Technical Memorandum 82706

Universal Binding Energy Relations in Metallic Adhesion

J. Ferrante
Lewis Research Center
Cleveland, Ohio

and

J. R. Smith
General Motors Research Laboratories
Warren, Michigan

and

J. H. Rose
Iowa State University
Ames, Iowa

Prepared for the
Aspects Microscopiques de l'Adhesion et de le Lubrification
sponsored by Société Chimie Physique
Paris, France, September 14–18, 1981

NASA

UNIVERSAL BINDING ENERGY RELATIONS IN METALLIC ADHESION

J. FERRANTE
National Aeronautics and Space Administration, Lewis Research Center,
Cleveland, Ohio U.S.A. 44135

J. R. SMITH
General Motors Research Laboratories, Warren, Michigan U.S.A. 48090

J. H. ROSE
Ames Laboratory, Iowa State University, Ames, Iowa U.S.A. 50011

ABSTRACT

Rose, Ferrante, and Smith (ref. 7) have discovered scaling relations which map the adhesive binding energy of Ferrante and Smith (ref. 6) onto a single universal binding energy curve. The energies in ref. 6 are calculated for all combinations of Al(111), Zn(0001), Mg(0001), and Na(110) in contact. The scaling involves normalizing the energy to the maximum binding energy and normalizing distances by a suitable combination of Thomas-Fermi screening lengths. A simple mathematical expression is found to accurately represent the universal curve, $E^*(a^*) = -(1 + \beta a^*) \exp(-\beta a^*)$ where E^* is the normalized binding energy, a^* is the normalized separation, and β is the fitting parameter. Rose et al. (ref. 7) have also found that the calculated cohesive energies of K, Ba, Cu, Mo, and Sm scale by similar simple relations suggesting the universal relation may be more general than for the simple free electron metals for which it was derived. In this paper we outline these results and discuss them in relation to topics of interest in adhesion, friction, and wear.

INTRODUCTION

An important aspect of friction and wear of metals is the nature of the adhesive force between the surfaces. Bowden and Tabor (ref. 1) have used adhesion between metals to explain parts of the friction and wear process. Of particular interest in these processes is the physical nature of the forces in dissimilar metal contacts.

There have been numerous attempts to postulate the nature of these forces but few model calculations. For example, adhesion between dissimilar metals was explained in terms of solubility (ref. 2) but without accompanying model calculations. Buckley (ref. 3) has shown that metals with low mutual solubility can have higher adhesion than those with high solubility.

This lack of model calculations has occurred because of the theoretical difficulties involved in treating solid surfaces. In the past decade the electron density functional formalism of Hohenberg, Kohn and Sham (ref. 4) have been used to successfully calculate the surface energies (ref. 5) of simple metals. Ferrante and Smith (ref. 6) recently applied this formalism to the problem of metallic adhesion for both similar and dissimilar metals in contact. Rose, Ferrante and Smith (ref. 7) found that scaling laws exist which map these results onto a universal adhesive energy curve. In this paper, we discuss the results of these calculations and their implications to a more general category of materials, the transition metals, and then summarize the current state of adhesion theory.

USE OF KOHN-SHAM FORMALISM FOR ADHESION CALCULATIONS

The calculational formalism and methods used for obtaining self-consistent interface electronic structure will now be presented. A much more extensive description is given in refs. 6 and 8, particularly of numerical techniques.

The adhesive interaction energy, E_{ad}, between two metal surfaces is a function of the distance between the two surfaces, a (see Fig. 1). E_{ad} is defined as the negative of the amount of work necessary to increase the separation from a to ∞ divided by twice the cross-sectional area A. Thus

$$E_{ad} = [E(a) - E(\infty)]/2A, \tag{1}$$

where E is the total energy. For identical metals, E_{ad} is the negative of the surface energy when a is at the energy minimum.

According to the density functional formalism of Hohenberg, Kohn, and Sham, (ref. 4) the total energy is given by (atomic units are used throughout unless otherwise specified)

$$E\{n(\vec{r})\} = \int v(\vec{r})n(\vec{r})d\vec{r} + \frac{1}{2}\sum_{i\neq j}\frac{z_i z_j}{R_{ij}} + F\{n(\vec{r})\}, \tag{2}$$

$$F\{n(\vec{r})\} = T_s\{n(\vec{r})\} + \frac{1}{2}\iint \frac{n(\vec{r})n(\vec{r}')}{|\vec{r} - \vec{r}'|}\, d\vec{r}\,d\vec{r}' + E_{xc}\{n(\vec{r})\} \tag{3}$$

$v(\vec{r})$ is the ionic potential, and $n(\vec{r})$ is the electron number density. The first two terms in Eq. (2) are the electron-ion and ion-ion interaction energies, respectively. z is the ionic charge and R_{ij} is the distance between ion core nuclei (there is no ion core overlap in the systems considered here). $T_s\{n(\vec{r})\}$ is the kinetic energy of a system of noninteracting electrons with the same density $n(\vec{r})$, the next term is the classical electron-electron interaction energy, and E_{xc} is the exchange-correlation energy.

For metals like Zn, Mg, Al, and Na, the jellium model (Fig. 1) is a good zeroth-order approximation, and the difference between the total pseudopotential and the potential due to the jellium is small for the closest packed plane. Thus for a given separation a, one obtains E to a first-order perturbation approximation as

$$E\{n(\vec{r})\} = A\int v_j(y,a)n(y,a)dy + \frac{1}{2}\sum_{i\neq j}\sum \frac{z_i z_j}{R_{ij}} + F\{n(y,a)\}$$

$$+ A\int \delta v\,(y,a)n(y,a)dy \tag{4}$$

where v_J is the potential produced by the jellium, y is the direction normal to the surfaces, and δv is the average, over planes parallel to the surface, of the difference in potential between an array of pseudopotentials and the jellium. Following Lang and Kohn (ref. 5) the Ashcroft pseudopotential is used:

$$v_{ps}(r) = \begin{cases} 0, & r < r_c \\ -z/r, & r > r_c \end{cases} \tag{5}$$

where r_c is determined empirically and is close to the ion core radius. The electron number density is obtained from a set of self-consistent equations.

The Schroedinger equation:

$$\left[-\frac{1}{2}\frac{d^2}{dy^2} + v_{eff}(n;y)\right]\psi_k^{(i)}(y) = \frac{1}{2}\left(k^2 - k_F^2\right)\psi_k^{(i)}(y) \tag{6}$$

where

$$v_{eff}(n;y) = \phi(y,a) + \frac{\delta E_{xc}\{n(y,a)\}}{\delta n(y,a)}$$

$$n(y,a) = n_L(y,a) + n_R(y,a)$$

$$n_L(y,a) = \frac{1}{4\pi^2} \int_0^{k_{FL}} dk \left| \phi_k^L(y) \right|^2 k_{FL}^2 - k^2$$

and

$$n_R(y,a) = \frac{1}{4\pi^2} \int_0^{k_{FR}} dk \left| \psi_k^R(y) \right|^2 k_{FR}^2 - k^2$$

and with Poisson's equation

$$\frac{d^2\phi(y,a)}{dy^2} = -4\pi[n(y,a) - n_+(y)] \tag{7}$$

$\phi(y,a)$ is the electrostatic potential $n_+(y)$ is the jellium density (Fig. 1) k_F is the Fermi wave vector magnitude and $\psi_k^{(i)}(y)$ is the wave function ($i = L, R$; i.e., left and right). The calculation is broken up into two regions, below the conduction band of the less dense metal, and above it where the solutions are doubly degenerate.

It is useful to combine the first two terms of Eq. (4) along with the classical electron-electron interaction term of $F\{n(y,a)\}$ as follows:

$$-\frac{1}{2} A \int \rho(y,a)\phi(y,a)dy + W_{int} \tag{8}$$

where $\rho(y,a)$ is the net charge density of the zeroth-order jellium solution. W_{int} is the exact difference between the ion-ion and the jellium-jellium interaction. It is shown in ref. 9 that W_{int}/A is negligible unless the facing planes are in registry, i.e., commensurate. In this calculation, we assume incommensurate adhesion ($W_{int} = 0$), since registry is not obtained with dissimilar metals in contact without corresponding loss of energy due to strains in the lattice which would be difficult to evaluate.

The exchange-correlation energy E_{xc} is written in the local-density approximation (LDA),

$$E_{xc}\{n(\vec{r})\} = \int n(\vec{r})\epsilon_{xc}(n(\vec{r}))d\vec{r} \tag{9}$$

where $\epsilon_{xc}(n(r))$ is the exchange-correlation energy of a uniform electron gas of number density $n(r)$. We use Wigner's interpolation formula for the correlation energy and the Kohn-Sham exchange energy.

It remains to specify the kinetic-energy functional of Eq. (3):

$$T_s\{n(y,a)\} = A \int t_s\{n(y,a)\}dy \tag{10}$$

where

$$t_s\{n(y,a)\} = \sum_{i=1}^{2} \sum_{\substack{k,k_x,k_z \\ (occ.)}} \left(k^2 + k_x^2 + k_z^2\right)\left|\psi_k^{(i)}(y)\right|^2$$

$$+ [v_{eff}(n;\pm\infty) - v_{eff}(n;y)]n(y,a) \qquad (11)$$

The sum is over all occupied states. The summation index i again refers to degenerate wave functions as in Eq. (6). In ref. 6, an expression for $T\{n(y,a)\} - T_s\{n(y,0)\}$ is presented which is based on kinetic-energy densities in the interface region. We find this approach more natural for our problem, as it is the interface region in which the large changes in kinetic energy density occur upon adhesion.

The results of this calculation for all dissimilar combinations of Al(111), Zn(0001), Mg(0001) and Na(110) are shown in Fig. 2. As can be seen there is a wide variation of shapes and binding energies and the curves look very similar to binding energy curves for diatomic molecules.

Scaling rules for adhesive energies

The calculations needed to obtain the results of Fig. 2 are quite difficult and time-consuming. It is of interest, therefore, to look for some general similarities between these curves which may generalize the results. Rose, et al. (ref. 7) have found such scaling laws. It will now be shown that the curves of Fig. 2, as well as those of the identical metal contacts (ref. 6) (Al(111) - Al(111), etc.), can be simply scaled into a universal curve. This scaling is motivated by the expectation that metals having shorter screening lengths would have adhesive energy curves which rise faster with separation. That is, the metals would screen the disturbances caused by creating the surface over a shorter distance. This suggests that for identical metal contacts the separation is scaled by the Thomas Fermi screening length $\lambda = (9\pi/4)^{1/3} r_s^{1/2}/3$ au, where the bulk electron density $n_+ = 3/4\pi r_s^3$. When we encounter bimetallic contacts as represented in Fig. 1, a length scaling appropriate to both metals must be considered. In that case, we chose to scale by an arithmetic average, $(\lambda_1 + \lambda_2)/2$. The energy amplitude was scaled by its equilibrium value, $\Delta E \equiv E_{ad}(a_m)$ where a_m is the equilibrium separation. Explicitly

$$E_{ad}(a) = \Delta E\, E^*_{ad}(a^*) \qquad (12)$$

Here $E^*_{ad}(a^*)$ is the univeral adhesive energy function and $a^* = 2(a - a_m)/(\lambda_1 + \lambda_2)$.

Figure 3 shows the results of scaling the calculated adhesive energies. An analytical fit is given by $E^*_{ad} = -(1 + \beta a^*)\exp(-\beta a^*)$ with $\beta = 0.90$. The

universality of the scaled adhesive energy curve is truly remarkable. One can see that the results for all ten bimetallic contacts lie very close to the universal curve. This is true even though the bulk metallic densities in the various metals vary by a factor of eight.

It is important to understand how the fortunate result of a universal energy curve comes about. In the following, we attempt to provide a plausibility argument within the jellium model. First, we have found that solid-vacuum density distributions, $n(y)$ (ref. 10), scale rather accurately with λ. That is, there is, to a good approximation, a universal number density distribution $n^*(y - a/2)$ where

$$n(y - a/2) = n_+ n^*[\lambda^{-1}(y - a/2)] \tag{13}$$

Here $a/2$ is the coordinate of the jellium surface. There is a similar scaling for the Kohn-Sham effective one electron potential:

$$V_{eff}(y - a/2) = v_B\, v^*_{eff}[\lambda^{-1}(y - a/2)] \tag{14}$$

We were motivated to look for this scaling by the fact that the Thomas Fermi equation scales (refs. 11,12) exactly with y in units of λ. Secondly, we have found (ref. 6) that the total number density in the bimetallic interface is given to a fair - accuracy by a simple overlap of the corresponding solid-vacuum distributions. This, and the stationary property of $E[n]$ indicates that it would be a good approximation to use overlapping solid-vacuum number density and potential distributions.

Thus, in a first order perturbation approximation, we have for identical metal contacts:

$$E_{ad}(a) = (1/A) \int_{-\infty}^{\infty} n(y - a/2) v_{eff}\ (y + a/2)dy \tag{15}$$

Combining Eqs. (3) to (5), we have:

$$E_{ad}(a) = (1/A)(n_+ v_B) \int_{-\infty}^{\infty} n^*(y - a^*/2) v^*_{eff}(y + a^*/2)dy \tag{16}$$

The integrand in Eq. (16) is independent of r_s. The constants in front of the integral are independent of a, and thus Eq. (16) scales exactly as we scaled the adhesive energy curve to give Fig. 3. Although our plausibility argument is restricted to jellium interfaces, we note that the calculated adhesive energies include the ion-ion term exactly for a rigid lattice model and the electron-ion term in first order perturbation theory.

DISCUSSION

There are several topics of importance in metallic adhesion: the nature of the attractive forces, the range of such forces, and finally, are there any

generalizations that can be found? The work of Ferrante and Smith (ref. 6) indicates that electron sharing similar to covalent bonding in molecules is sufficient to give strong bonding. They also determine the magnitudes of such forces for several simple metals (table 1). These results also establish that an approximate range for the forces is an interplanar spacing. Finally, Rose, Ferrante and Smith (ref. 7) have found scaling laws which generalize these results.

In metallic adhesion of real surfaces further considerations come to mind. First, real surfaces are not flat and consequently, how important are the strong forces compared to the weaker, long-range van der Waals forces? Next, the results of these theoretical calculations represent ideal strengths. Real contacts fail at conditions lower than at ideal strengths. Finally, metals used in most engineering applications are either transition metals or alloys.

Inglesfield (ref. 13) examined the problem of van der Waals vs. strong interaction forces using the calculations of Ferrante and Smith (ref. 9). He concluded that in spite of the fact that the strong forces only dominate at the positions of asperity contact, these strong interaction forces dominate the strength of the contact.

The fact that the strength of real contacts is dominated by defect structures and the mechanical properties of the solids is an issue that ultimately must be addressed. Also, these results apply for brittle fracture; however, metals will undergo ductile extention before fracture. Since adhesion and other contact processes are complicated combinations of physical and mechanical properties, each part of the process must be understood independently. This study has been carried out in this spirit. The results of table I, however, contain some aspects of these considerations. A question of interest is whether a dissimilar contact is weaker, stronger or in-between contacts between the same metal. The first column in table I (labeled Wint = 0) gives the binding energy of a contact when perfect registry is not obtained. Perfect registry can only be obtained when the same crystallographic planes of the same metal are in contact. A more complete discussion of this issue is given in ref. 9. The second column gives the binding energy in the ideal case of perfect matching of planes which doesn't occur in a real contact. Examining table I, it can be seen that the interfacial energy is slightly lower than or comparable to the bulk energy except for the case of sodium, where the interface between sodium and any of the other metals is clearly stronger than the bulk. In a real contact, the two surfaces would probably distort to attempt to come into registry with the formation of defect chains to accomodate the distortions, thus modifying the interfacial energy. In general, the interfacial binding energy is comparable to the energy of the weaker partner in the different metal contacts examined.

A final concern with these results is the limitations of the calculations. The quasi-three-dimensionality of the adhesion calculations limits the reliability of the calculations to the densest packed planes of the simple metals.

Most engineering materials are transition metals. To properly handle transition metals theoretically would require extensive three-dimensional calculations which would be quite difficult at this stage. Yaniv (ref. 14) and Allan, Lannoo and Dobrzhinski (ref. 15) have applied the tight-binding approximation to the transition metal problem. Although these calculations probably give accurate trends, the approximations used make quantitative results questionable.

The question arises concerning whether the results are more general than for the simple metals examined. Recently, theoretical binding energy curves have become available for several bulk metals [Carlsson et al. (ref. 16) (Mo, K, and Cu) and Herbst (ref. 17) (Sm^{+2}, Sm^{+3}, and Ba)]. These total cohesive energy curves were calculated as a function of the separation between atoms for a uniformly dilated lattice. We characterize the density of the lattice in terms of the Wigner-Seitz radius, $r_{ws} = (3/4\pi n_A)^{1/3}$ where n_A is the atom density. As shown in Fig. 4, these quite disparate cohesive energy curves can be approximately scaled into a universal function, E_c^*, which is also defined in Eq. (12) if we replace E_{ad} by E_c everywhere. ΔE is the cohesive energy at the equilibrium spacing r_{wsm} and $a^* = (r_{ws} - r_{wsm})/\lambda$ where λ is again the Thomas-Fermi screening length. The value of r_s used to determine λ was determined by the equilibrium interstitial electron density (refs. 17,18). The binding energy of Mo, K, Ba, Sm $[4f\ (5d,6s)^2]$ and $Sm^{+3}[4f^2(5d,6s)^3]$ fall closely on a single curve with $\beta = 1.16$ where we have used the same analytic form as for the adhesive energies. The value of β differs from that appropriate for adhesive energies presumably in part because all atoms change their positions in the bulk cohesive energy calculations while the adhesive energy curves assume that atomic planes are moved rigidly. The results for Cu has the same shape, but a somewhat different β than the other metals. We do not understand this variation.

The cohesive energy calculations of Carlsson et al. (ref. 16) (ASW density functional theory) and Herbst (ref. 18) (relativistic Hartree-Fock) are quite different from each other and from the perturbative-density functional results of ref. 6 for E_{ad}. The nature of cohesive bonding in these metals is quite varied. Ba is a divalent band overlap metal; Sm is an f-electron metal; Mo and Cu have important d-band interactions; while K is a simple metal. That such different metals calculated in quite different ways fall on a single curve indicates the generality of the scaling relations. We note that the "tail" region of the screening charge distribution around metal ion cores can be represented by electron gas parameters. It is known that the screening charge density and potential in this region scale as $r_s^{1/2}$ to a fair approximation (ref. 19). Then the argument of Eqs. (13 to 15) applies to the long-range interaction of screened bulk ions with $\pm a/2$ referring to the relative lattice positions and y replaced by $\vec{r}$.

The use of the electron density at r_{ws} is reminiscent of the approach of Miedema et al. (ref. 20) whose work complements our own. They calculate equilibrium energies (e.g., heats of formation). We, on the other hand, use similar equilibrium quantities to determine the form of the binding energy-distance relation.

The plotted energies of Fig. 4 were computed for the same electronic configuration at all atomic separations as were the interface calculations. The adhesive energy scaling was illustrated for simple metals. However, the appearance of an analogous scaling relation for the bulk energy of transition metals indicates that the adhesive energy scaling may well extend beyond simple metals.

In conclusion we have discovered scaling relations which map adhesive energies onto a universal binding energy curve. Similar scalings for cohesive energies for a wide range of metals suggest that this relation may apply to more than just the simple metals. Finally, a simple analytic energy-separation scaling relation is provided which may be of use in practical analysis of contacts.

REFERENCES

1. D. Tabor, in J.M. Blakely (Ed.), Surface Physics of Materials, Vol. 2, Academic, New York, 1975, ch. 10.
2. E. Rabinowicz, Friction and Wear of Materials, Wiley, New York, 1965.
3. D.H. Buckley, J. Colloid Interface Sci., 58 (1977) 36-53.
4. W. Kohn and L.J. Sham, Phys. Rev., 140 (1965) A 1133-1138.
5. N.D. Lang and W. Kohn, Phys. Rev., B 1 (1970) 4555-4568. R. Monnier and J.P. Perdew, Phys. Rev., B 17 (1978) 2595-2611.
6. J. Ferrante and J.R. Smith, Phys. Rev. B 19 (1979) 3911-3920. J. Ferrante and J.R. Smith, Bull. Am. Phys. Soc., 26 (1981) 428.
7. J.H. Rose, J. Ferrante and J.R. Smith, Phys. Rev. Lett. 47 (1981) 675-678.
8. J. Ferrante, NASA TM-78890, 1978.
9. J. Ferrante and J. R. Smith, Surf. Sci., 38 (1973) 77-92.
10. J.R. Smith, J. Ferrante, and J.H. Rose, to be published.
11. B. Mrowka and A. Recknagel, Phys. Z. 38 (1937) 758-765.
12. S.C. Ying, J.R. Smith and W. Kohn, J. Vac. Sci. Technol., 9 (1972) 575-578.
13. J.E. Inglesfield, J. Phys. F, 6 (1976) 687-701.
14. A. Yaniv, Phys. Rev. B, 17 (1978) 3904-3918.
15. G. Allan, M. Lannoo and L. Dobrzynski, Philos. Mag., 30 (1974) 33-45.
16. A.E. Carlsson, C.D. Gelatt, Jr., and H. Ehrenreich, Phil. Mag. A, 41 (1980) 241-250. (An ASW calculation).
17. We would like to thank J.F. Herbst for giving us access to his unpublished calculations of Sm and Ba. In this case, r_s was determined from the electron density at the cell boundary.
18. V.L. Moruzzi, J.F. Janak and A.R. Williams, Calculated Electronic Properties of Metals, Pergamon, New York, 1978.

19. See e.g., S. Raimes, Wave mechanics of electrons in metals, Interscience, New York, 1961, esp. Eq. 10.85, p. 305.
20. A.R. Miedema, R. Boom and F.R. DeBoer, J. Less Common Met., 41 (1975) 283-298. A.K. Miedema, Phillips Tech. Rev., 36 (1976) 217-231.

TABLE I.
Binding energy comparison. All energy values taken from the minimum in the adhesive energy plots (see figs. 3 and 4)

Metal combination	Binding energy	
	$W_{int} = \rho$, ergs/cm^2	Perfect registry
Al(111)-Al(111)	490	715
Zn(0001)-Zn(0001)	505	545
Mg(001)-Mg(0001)	460	550
Na(110)-Na(110)	195	230
Al(111)-Zn(0001)	520	
Al(111)-Mg(0001	505	
Al(111)-Na(110)	345	
Zn(0001)-Mg(0001)	490	
Zn(0001)-Na(110)	325	
Mg(0001)-Na(110)	310	

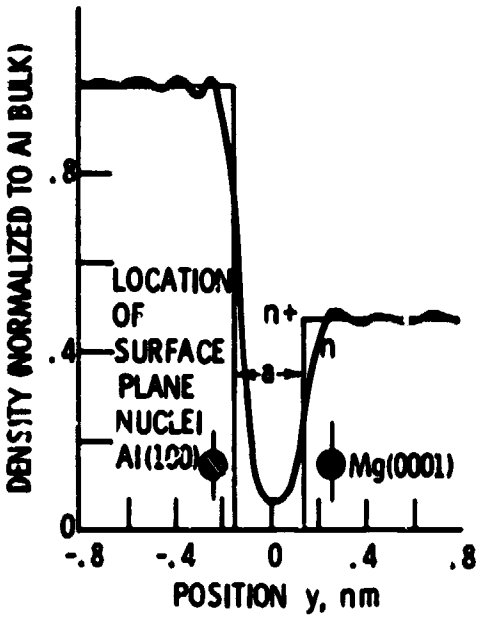

Figure 1. - Electron number density n and jellium ion charge density n_+ for an Al-Mg contact.

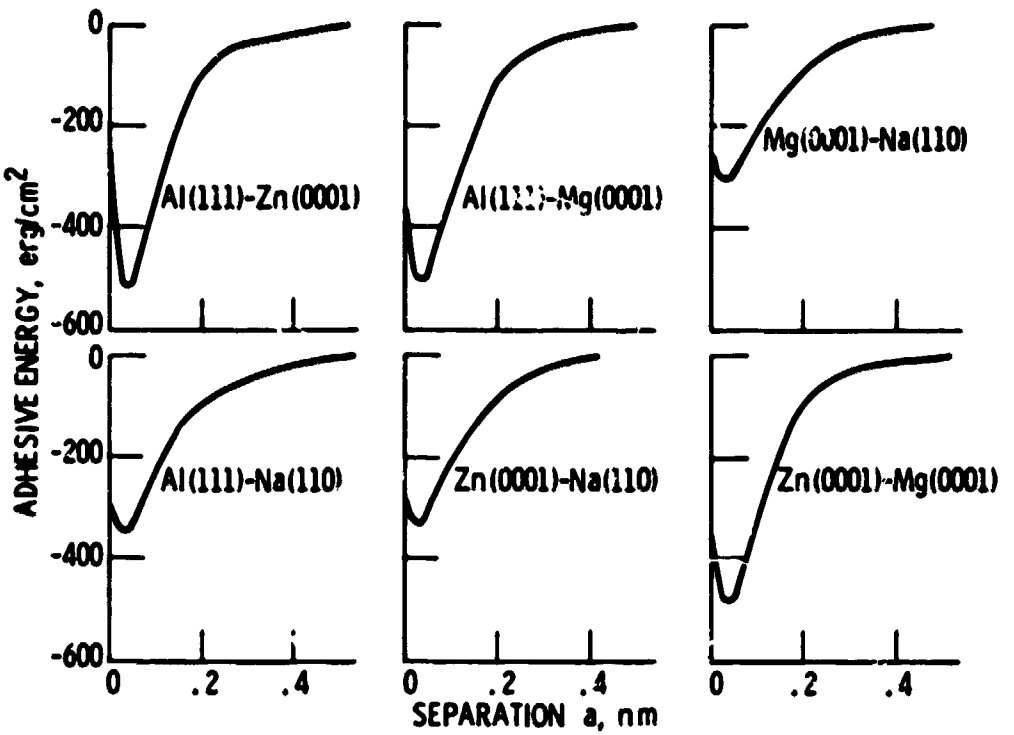

Figure 2. - Adhesive binding energy versus the separation a between the surfaces indicated.

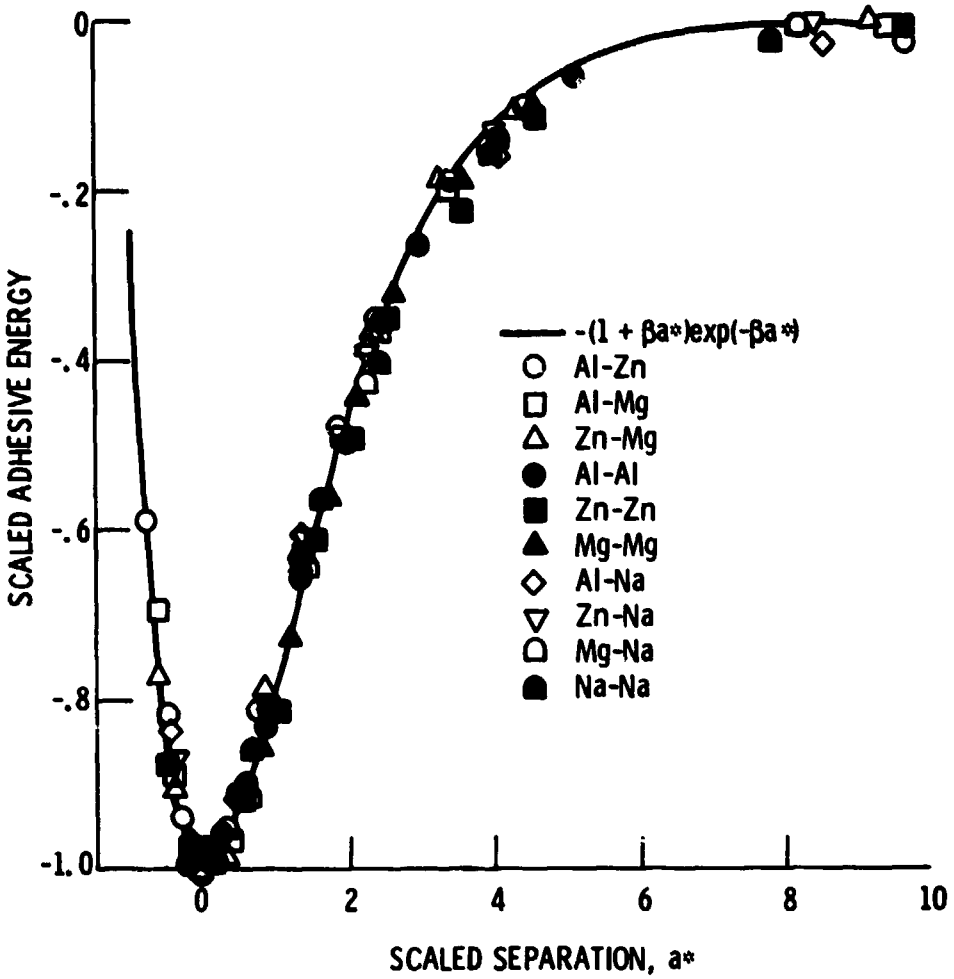

Figure 3. - Adhesive energy results from Fig. 1 above and Fig. 4 of Ref. 1 scaled as described in the text: $a^* = 2(a - a_m)/(\lambda_1 + \lambda_2)$.

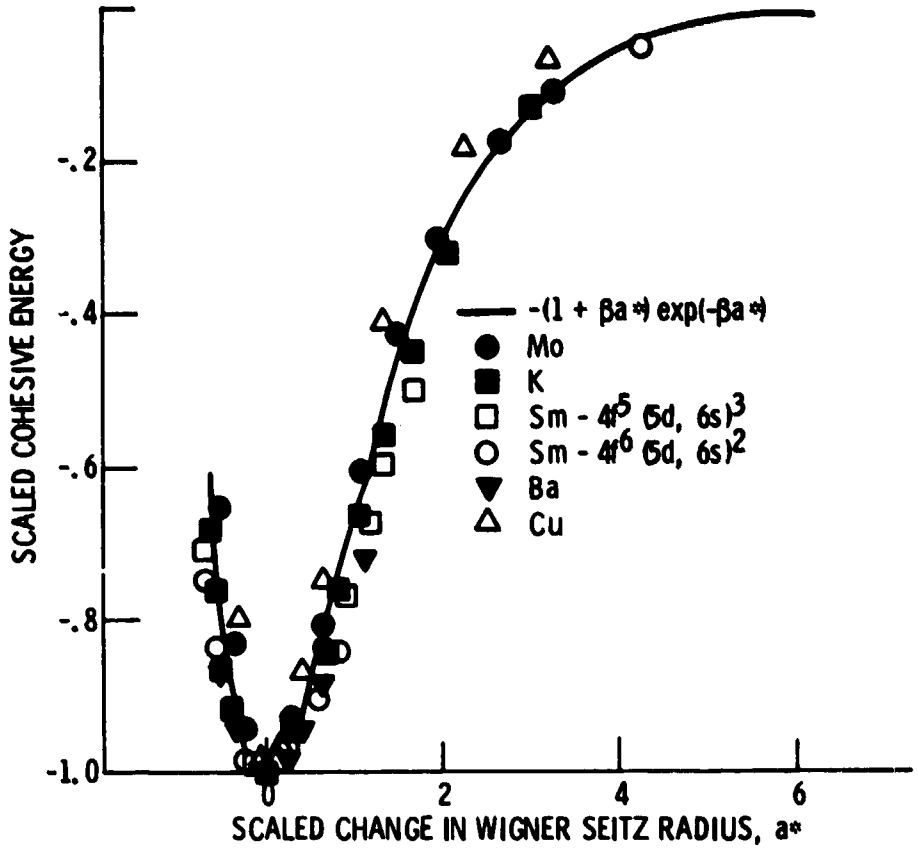

Figure 4. - Bulk energy of various metals scaled and described in the text: $a^* = (r_{ws} - r_{wsm})/\lambda$. A value of $\beta = 1.16$ was obtained by a least squares fit to the data.